ACS OMEGA

Article

Cite This: ACS Omega 2019, 4, 14560−14568

http://pubs.acs.org/journal/acsodf

Highly Sensitive in Vitro Diagnostic System of Pandemic Influenza A (H1N1) Virus Infection with Specific MicroRNA as a Biomarker

Jaewoo Lim,[†,‡] Jihyun Byun,[†] Kyeonghye Guk,[†,‡] Seul Gee Hwang,[†,‡] Pan Kee Bae,[§] Juyeon Jung,*[,†,‡] Taejoon Kang,*[,†,‡] and Eun-Kyung Lim*[,†,‡]

[†]BioNanotechnology Research Center, Korea Research Institute of Bioscience and Biotechnology (KRIBB), 125 Gwahak-ro, Yuseong-gu, Daejeon 34141, Republic of Korea

[‡]Department of Nanobiotechnology, KRIBB School of Biotechnology, University of Science and Technology (UST), 217 Gajeong-ro, Yuseong-gu, Daejeon 34113, Republic of Korea

[§]BioNano Health Guard Research Center, 125 Gwahak-ro, Yuseong-gu, Daejeon, 34141, Republic of Korea

Supporting Information

ABSTRACT: Several microRNAs (miRNAs) have been reported to be closely related to influenza A virus infection, replication, and immune response. Therefore, the development of the infectious-disease detection system using miRNAs as biomarkers is actively underway. Herein, we identified two miRNAs (miR-181c-5p and miR-1254) as biomarkers for detection of pandemic influenza A H1N1 virus infection and proposed the catalytic hairpin assembly-based in vitro diagnostic (CIVD) system for a highly sensitive diagnosis; this system is composed of two sets of cascade hairpin probes enabling to detect miR-181c-5p and miR-1254. We demonstrated that CIVD kits could not only detect subnanomolar levels of target miRNAs but also distinguish even single-base mismatches. Moreover, this CIVD kit has shown excellent detection performance in real intracellular RNA samples and confirmed results similar to those of conventional methods (microarray and quantitative real-time polymerase chain reaction).

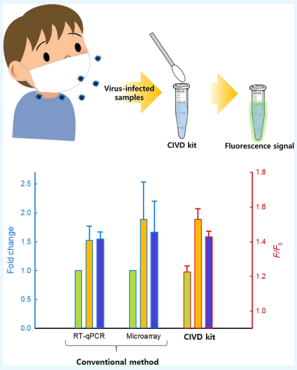

INTRODUCTION

The influenza virus is one of the major threats in modern public health. It mainly infects the upper respiratory tract and results in the massive release of inflammatory factors that lead to acute respiratory diseases.[1−3] Three influenza types (A, B, and C) are well known as flu pathogens. Among them, the most virulent pathogen is the type A influenza, which has various subtypes due to the combination of 18 hemagglutination proteins and 11 neuraminidase proteins, leading to seasonal epidemics and global pandemics.[4,5] Influenza virus spreads rapidly through transmission among humans, and influenza infection poses a serious threat to public health. According to a WHO report, approximately 50,000 people were affected by and 2,700 people died from pH1N1 virus infection in 2009 to 2010. Hence, clinical care, control, and prevention are very important in influenza infections.[6,7] Serological assays, such as the HA inhibition assay (HAI) and enzyme-linked immunosorbent assay (ELISA), are most commonly used to detect the influenza virus using antigen-specific antibody responses. Although these assays are simple and rapid, their sensitivity for influenza virus subtype identification is limited for practical virus diagnosis.[8] Nucleic acid-based tests (NATs), which are based on the polymerase chain reaction (PCR) technique, are a powerful approach for the identification of influenza virus subtypes. Reverse transcription PCR (RT-PCR) is the most traditional method for influenza virus diagnosis and is more sensitive than other immunoassays. However, this technique requires expensive instruments and involves tedious and complicated processes.[9−11] To alleviate these concerns, a rapid and sensitive diagnostic technique for infectious diseases needs to be developed. Recent findings report that several cellular miRNAs are closely associated with influenza A virus infection and replication, particularly the immune response to virus infections due to their aberrant expression. For example, miR-323, miR-491, and miR-654 inhibit the replication of the H1N1 influenza A virus by regulating the BAX inhibitor gene, and miR-200a directly regulates host immune response genes such as IFNAR1 and STAT2.[12−14] Thus, the distinctive expression patterns of miRNAs have been shown to be associated with various pathological conditions, and these miRNAs may be able to serve as biomarkers.[15−17] Furthermore, miRNAs related to influenza have been reported to be stably detected in serum and saliva samples.[18] However, detection of miRNA is not easy because of its intrinsic properties (21−23 nucleotides of short length and high homology) and low concentration in body fluids (serum and saliva).[19−21] Until now, northern blotting, microarray, and quantitative real-time PCR (qRT-PCR) have been widely used to detect miRNA, but these techniques have some drawbacks,

Received: June 17, 2019
Accepted: July 31, 2019
Published: August 26, 2019

DOI: 10.1021/acsomega.9b01790
ACS Omega 2019, 4, 14560−14568

Scheme 1. Highly Sensitive Detection of the Pathogenesis of pH1N1 Influenza A Virus Infection[a]

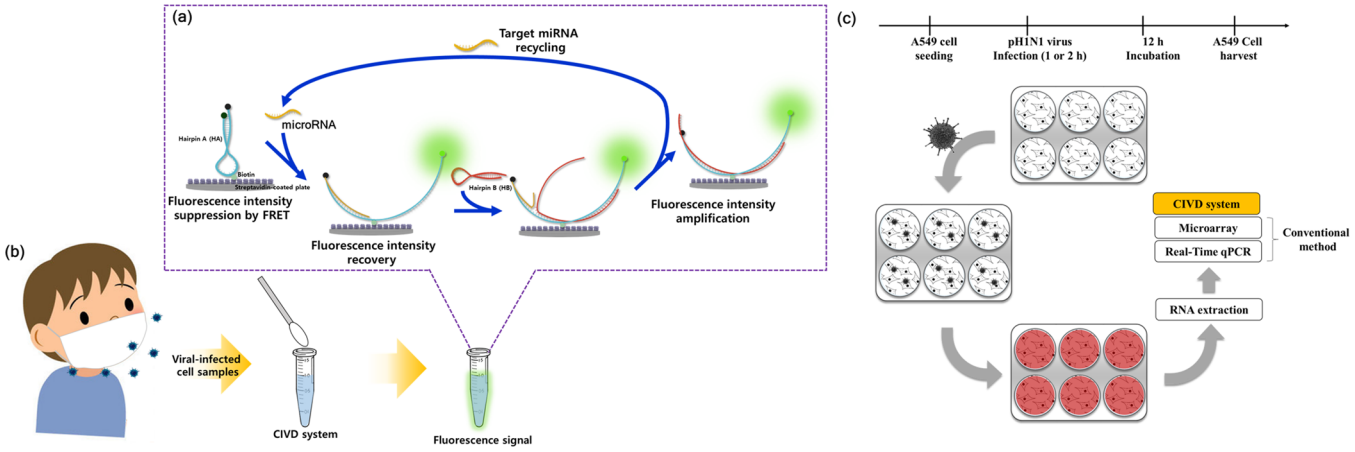

[a](a) Principle of miRNA detection based on catalytic hairpin assembly (CHA). (b) Collection of a liquid specimen from the viral-infected cells and fluorescence detection. (c) Illustration of the experimental procedure of microRNA detection from influenza virus-infected A549 cells

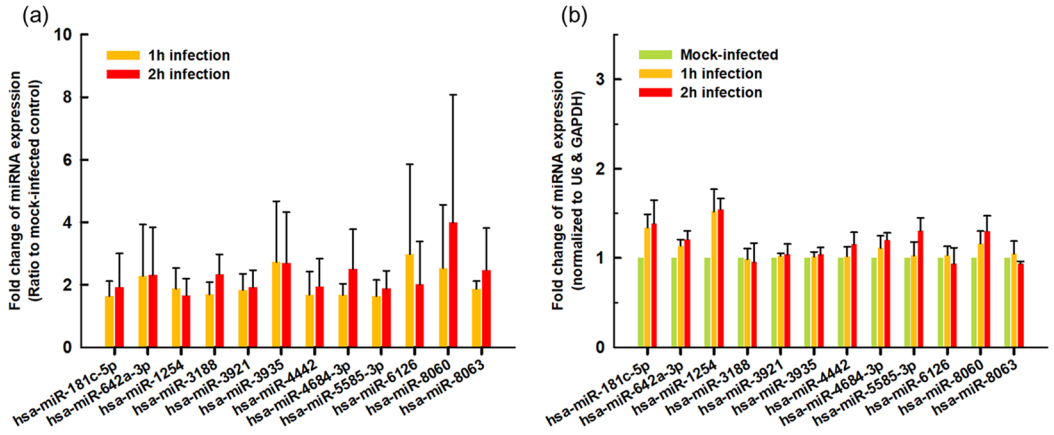

Figure 1. MicroRNA expression profiling. (a) Microarray analysis for miRNA was performed with RNA extracts from A549 cells 12 h postinfection with pH1N1 virus (MOI = 1) for 1 or 2 h. The fold changes were compared to those of mock-infected cells. (b) qRT-PCR analysis of the expression of miRNAs. The fold changes were normalized to U6 and GAPDH and calculated using $2^{-\Delta\Delta Cq}$.

including the need for expensive equipment, the time-consuming process, and the large sample volumes required.[22−28] To overcome these challenges, novel concepts based on nucleic acid amplification, such as rolling circle amplification (RCA),[29,30] catalytic hairpin assembly (CHA),[31,32] hybridization chain reaction (HCR),[33−35] and loop-mediated isothermal amplification (LAMP),[36] have been proposed. Among these strategies, CHA is a promising technique due to its remarkable features, such as its enzyme-free amplification, thermal cycle-free reaction, and low background signal. Selective binding catalyzes CHA performance, which is an entropy-driven reaction, initiates cross-opening of two metastable hairpin DNA probes and generates numerous signals.[22,37,38] In addition, the CHA technique is compatible with various reporting systems, such as fluorescent, colorimetric, and electrochemical signals, through immobilization.[39−42] In this study, we propose a CHA-based in vitro diagnostic system (CIVD system) for the rapid and sensitive detection of pH1N1 virus infection by accurate miRNA expression analysis. As shown in Scheme 1, we designed two types of probes, hairpin A (HA) and hairpin B (HB), and used them to establish an in vitro diagnostic platform where the HA is labeled with biotin fixed on a streptavidin (SA)-coated sensor plate, and a fluorescence and quencher at each end report the signal. After the target miRNA binds with HA and generates a fluorescent signal, HB hybridizes with open sequences of HA to release the bound miRNA. Released target miRNA is reused as a fuel that can activate the fluorescence signal by opening another HA. Moreover, we identified two species of miRNA, miR-181c-5p and miR-1254, as potential biomarkers of pH1N1 virus infection by both microarray and qRT-PCR approaches.[43] To achieve high reliability of the proposed CIVD system, we designed a dual module composed of cascade hairpin probes for detecting miR-181c-5p and miR-1254.[44] Using our CIVD system, we demonstrated excellent diagnostic performance using real cellular RNA molecules and the ability to specifically identify pH1N1 virus infection.

RESULTS AND DISCUSSION

Exploration of miRNA as a Novel Biomarker. To develop an early diagnosis system of pH1N1 virus infection using miRNA as a biomarker, we first analyzed the miRNA expression profile in A549 cells infected with pH1N1 virus. A549 cells were infected with 1 MOI of pH1N1 virus for 1 or 2 h and then incubated for 12 h p.i.[45,46] An overview of the experimental procedure is illustrated in Scheme 1c. For global

DOI: 10.1021/acsomega.9b01790
ACS Omega 2019, 4, 14560−14568

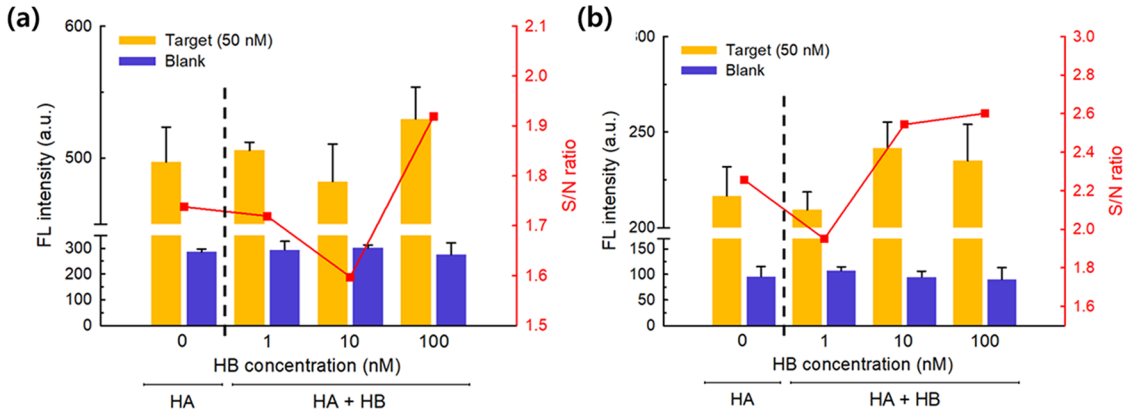

Figure 2. Evaluation of the concentration of HB for (a) miR-181-5p and (b) miR-1254. The signal-to-noise ratio (S/N ratio) was calculated with the intensity of the target per the intensity of blank.

screening of miRNA expression in influenza A virus-infected cells, we analyzed miRNA expression profiling from virus-infected cells using microarray technology. This microarray was performed three times on the Affymetrix GeneChip miRNA 4.0 and profiled 30,424 species of mature miRNAs (all organisms). From this analysis, we compared miRNA expression levels in A549 cells that infected the pH1N1 virus to mock-infected A549 cells as a control. Among the mature miRNA species, we studied 1919 human miRNAs (Figure S1a). As a result, we found that 19 and 46 miRNAs were upregulated with a 1.5-fold increase compared to the control when infected with influenza virus for 1 and 2 h, respectively (Figure S1b). In particular, 12 miRNAs were reported to be overexpressed at both time criteria (Figure 1a and Figure S1c). Thus, we considered the 12 miRNAs as potential biomarkers for the diagnosis of pH1N1 virus infectious diseases. To confirm the expression level of the 12 selected miRNAs, we used qRT-PCR (Figure 1b). Among the miRNAs displayed in the qRT-PCR results, miR-181c-5p and miR-1254 were significantly upregulated. In several previous studies, miRNA-1254 has been implicated not only in cancer, such as non-small-cell lung cancer (NSCLC),[47,48] but also in pH1N1 infection,[49] and miRNA-181c-5p has been reported to be associated with the immune response[50] and control of viral replication in pulmonary infectious diseases such as the Hendra virus (HeV) and the Nipah virus (NiV).[51] Since the aberrant expression (over-/low expression) of miRNA can indicate one or more diseases, we designed a dual-module diagnostic platform for the reliable diagnosis of infectious diseases using both miR-1254 and miR-181c-5p as diagnostic markers.[52]

Preparation of the Hairpin Probes for miRNA Detection. We designed hairpin probes (HA) that can generate a fluorescence signal when the probe detects miR-181c-5p and miR-1254 and catalytic hairpin probes (HB) that induce signal amplification through an entropy-driven cascade reaction (Table S1). Scheme 1 illustrates the mechanisms of CHA-based fluorescence amplification for miRNA detection. Both metastable hairpin probes (HA and HB) were employed in the CHA process. In the absence of a target miRNA, these probes stably formed a hairpin structure due to the complementary sequence at the end of each probe. This is because the stem sequences of the probes were longer than those of the other probes so that each probe remained thermodynamically stable and did not hybridize with other probes. HA was labeled with biotin at the loop, so it was immobilized on the SA-coated sensing plate by the avidin−biotin interaction, and each end was labeled with a fluorescence dye (FAM) and a quencher (BHQ1).[53,54] Therefore, during hairpin formation, the fluorescence of the HA was decreased with quencher molecules due to the Förster resonance energy transfer (FRET) effect. In the presence of a target miRNA, HA hybridized with the target miRNA and opened its folding structure. When the HA and target miRNA hybridized, the complementary sequence of HA to another HB was exposed. HB docked on the HA−target complex and liberated the target. The released target miRNA was then hybridized to another HA and introduced a new CHA circuit. To achieve optimal performance for miRNA detection based on hairpin probes, first, the concentration of the magnesium ion (Mg^{2+}) was optimized. Salt, including Mg, K, and Na, is a crucial factor in DNA thermodynamics because it regulates the Watson−Crick binding affinity.[55] Unintended hybridizing of HA and HB can occur with high noise and is an obstacle to accurate detection of miRNA in the CHA-based technique. Therefore, we looked for the optimal buffer conditions at various Mg^{2+} concentrations. As shown in Figure S2, the signal-to-noise ratio (S/N ratio) at 12.5 mM showed the highest signal in the targets, but that of the control also increased. Although 5 mM is lower than the other conditions in the targets, little noise was observed in the control. Therefore, 5 mM was chosen as the optimal Mg^{2+} concentration. To further enhance the immobilization, we optimized the concentration of SA and bHA. First, various SA concentrations (0.1, 0.2, 0.5, and 1 μg/well) were coated onto the well plates followed by incubation with unannealed 50 nM bHA to measure the fluorescence signal. After washing the unbound residue, the fluorescence of bHA was measured when there was no target miRNA (Figure S3a). Its fluorescence intensity increased as the concentration of SA increased. Hence, a 1 μg/well concentration of SA was chosen as the optimal condition. Then, we determined the optimal bHA concentration by measuring the fluorescence intensity of bHA by treating various concentrations on optimized SA-coated plates. The fluorescence intensity was highest at 0.1 μM bHA, but the signal output decreased at more than 0.1 μM (Figure S3b). This is due to the self-quenching effect of excess bHA, which can lead to inaccurate diagnostic results. As a result, we chose 0.1 μM as the appropriate concentration of bHA. We prepared a hairpin probe-based miRNA detection system that

DOI: 10.1021/acsomega.9b01790
ACS Omega 2019, 4, 14560−14568

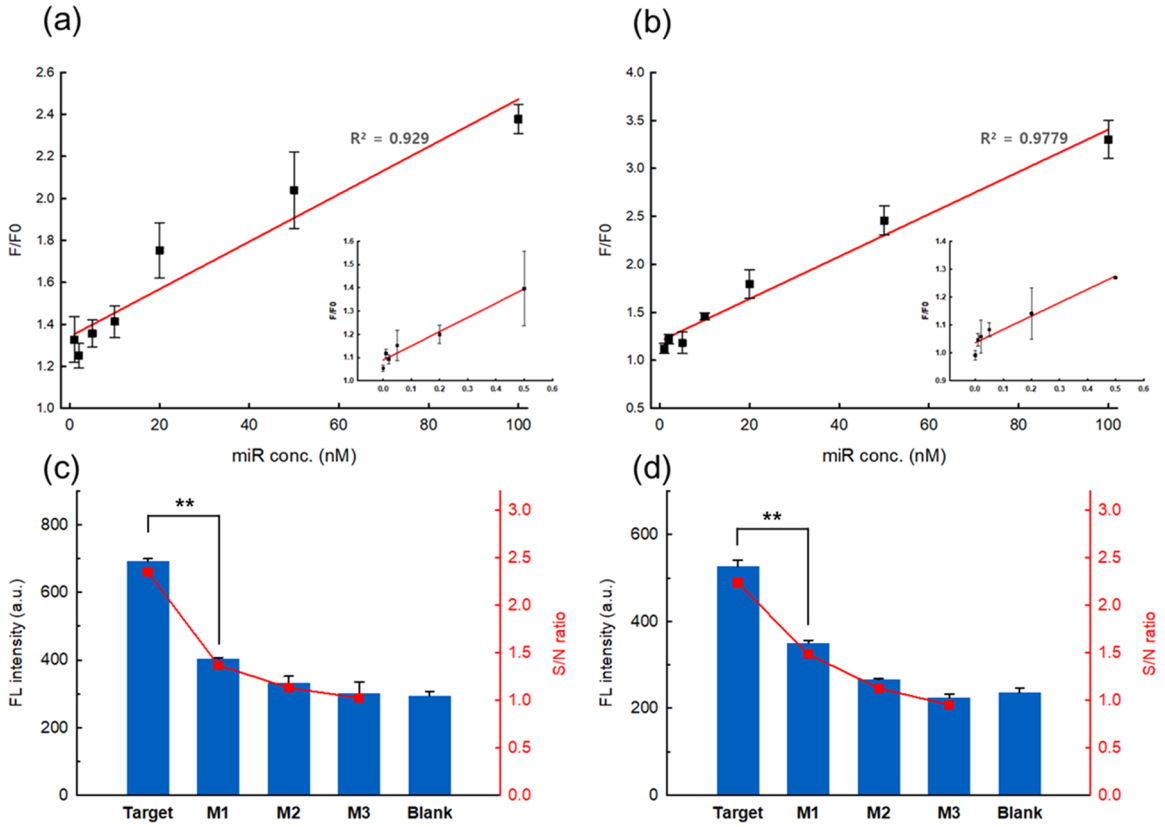

Figure 3. Sensitivity and selectivity. Fluorescence recovery ratio (F/F_0) of (a) miR-181c-5p and (b) miR-1254 analysis in the presence of various concentrations of the synthetic target: 1 nM−100 nM and 10 pM−0.5 nM (inset). Selectivity investigation of the miRNA detection method for (c) miR-181c-5p and (d) miR-1254 with 50 nM of different miRNA samples: M1, single-base mismatch miRNA; M2, double-base mismatch miRNA; M3, triple-base mismatch miRNA; blank, absence of the target miRNA. The fluorescence recovery ratio equation is $F_{\text{at 120 min}}$ per $F_{\text{at 0 min}}$ (**p < 0.005).

can be used as an in vitro diagnostic kit for the pH1N1 virus infectious disease and evaluated the detection performance of this kit. Based on the above results, SA (1 μg/well) and bHA (0.1 μM) were immobilized on a well plate, and HBs were added to the wells at various concentrations (0, 1, 10, and 100 nM). Then, 50 nM target miRNA was added to the prepared detection wells, and fluorescence intensity was measured every 20 min for 2 h (Figure 2a,b and Figure S4a,b). In the presence of the target miRNA, the fluorescence intensity significantly increased due to HA and target binding. However, in the miR-181c-5p analysis, the fluorescence signal at 1 nM HB and 10 nM HB was similar to that of the HA-coated well, but at 100 nM HB, the fluorescence signal increased compared to that in the other conditions. Although the fluorescence signal of 1 nM HB was lower than that of HA alone in the miR-1254 analysis, both the 10 nM HB and 100 nM HB conditions showed high signal increases. As a result of each analysis, we confirmed that the S/N ratio reached its maximum at 100 nM HB (Figure S4c,d), demonstrating that the optimized HB concentration was 100 nM. Moreover, even though the concentration of HB increased, the fluorescence intensity of the blank (absence of target) remained stable. These results indicated that the hairpin-forming metastable probes were intact until target detection, and the proposed strategy was well optimized and ready to test. Three types of inconsistent (mismatch) sequences with the target miRNA sequences were used as controls (M1: one mismatch with the target miRNA sequence, M2: two mismatches with the target miRNA sequence, and M3: three mismatches with the target miRNA sequence). Furthermore, fluorescence intensities were measured for 2 h after treatment at various concentrations of each target miRNA (miR-181c-5p and miR-1254). As shown in Figure 3a,b, the F/F_0 value (F/F_0, F: fluorescence intensity at 120 min and F_0: fluorescence intensity at 0 min) increases with increasing concentration of target miRNA from 1 to 100 nM (inset: 10 pM−0.5 nM concentration range). The F/F_0 value shows a strong linear correlation between the target miRNA concentrations and the fluorescence signal with correlation coefficients of R^2 = 0.929 and 0.9779, respectively. The limit of detection (LOD) was calculated based on 3σ/slope (σ = standard deviation of blank, n = 3) and estimated 0.06 nM (miR-181c-5p) and 0.11 nM (miR-1254). Therefore, we can confirm that dual-module CIVD systems are capable of quantifying miRNAs at subnanomolar levels and can be used for the highly sensitive detection of pH1N1 virus infections. The selectivity of our system was evaluated by using control miRNAs (M1, M2, and M3) and a blank (only buffer). As shown in Figure 3c,d, the fluorescence intensity of the target miRNA (50 nM) significantly increased 2.5-fold compared to the blank. However, the M1, M2, and M3 conditions showed weak fluorescence intensity (M1-181c-5p: 1.3-fold, M2-181c-5p: 1.1-fold, M2-181c-5p: 1.0-fold, M1-1254: 1.5-fold, M2-1254: 1.2-fold, and M3-1254: 0.9-fold), and fluorescence signals did not increase as the mismatch sequence increased due to nonspecific binding. Although similar fluorescence intensities were measured in all control groups (M1, M2, and

DOI: 10.1021/acsomega.9b01790
ACS Omega 2019, 4, 14560−14568

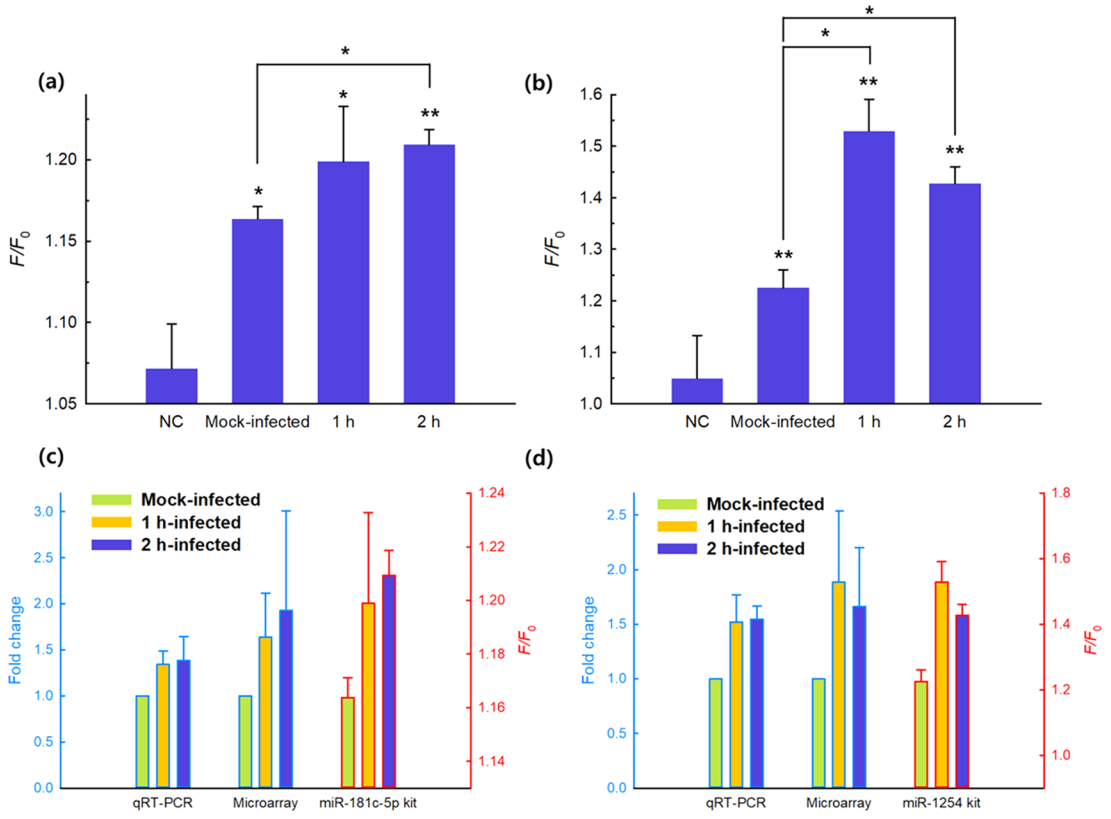

Figure 4. Observation of the fluorescence response with a real RNA sample (1 μg/well). The fluorescence recovery ratio (F/F_0) was monitored by (a) the miR-181c-5p kit and (b) the miR-1254 kit for 2 h. The total RNA was isolated from the negative control (NC; only hairpin probes), the mock-infected cells (no virus treated), 1 h-infected cells, and 2 h-infected cells in the A549 cell line with pH1N1. Performance comparison for (c) miR-181c-5p and (d) miR-1254 expression analysis by qRT-PCR, microarray, and the CIVD system (*p < 0.05, **p < 0.005).

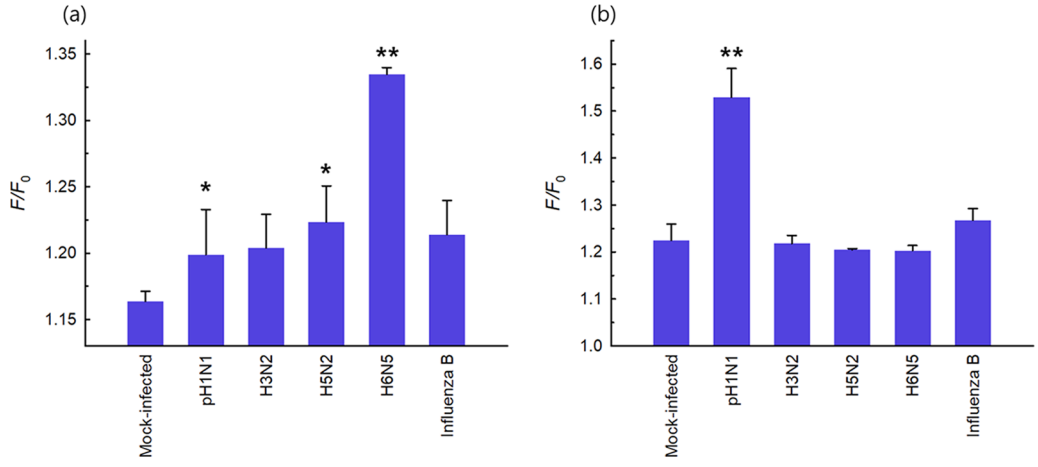

Figure 5. Observation of the fluorescence response with miRNA in A549 cells infected with various influenza viruses, including influenza A (pH1N1, H3N2, H5N2, and H6N5) viruses and influenza B virus. Each fluorescence intensity ratio (F/F_0) was monitored by (a) the miR-181c-5p kit and (b) the miR-1254 kit for 2 h (*p < 0.05, **p < 0.005).

M3) compared to the blank, these intensities were considered to be unaffected by the selectivity evaluation of miRNA detection. These comparisons confirm that only perfectly complementary miRNA can initiate the CHA procedure as a trigger for fluorescence signal amplification.

Performance Evaluation Using Real Samples (RNA) Extracted from Virus-Infected Cells. After the characterization, our CIVD kit was evaluated using RNA isolated from influenza virus-infected A549 cells as real samples. As described above, we prepared detection wells containing bHA and HB capable of detecting two target miRNAs (miR-181c-5p and miRNA 1254) and added 1 μg of RNA to each well and measured the fluorescence intensities. As shown in Figure 4, the fluorescence intensity ratio (F/F_0) of the miR-181c-5p and miR-1254 detection kits was observed for 2 h (Figure 4a,b). The miR-181c-5p level in infected cells significantly increased by 47% (1 h) and 61% (2 h) compared with the levels in mock-infected cells (control). Likewise, the miR-1254 level in infected cells was 161% (1 h) and 107% (2 h) higher in the fluorescence recovery ratio. These results

DOI: 10.1021/acsomega.9b01790
ACS Omega 2019, 4, 14560−14568

showed good agreement with the results of the microarray and qRT-PCR analysis (Figure 4c,d). In addition, we evaluated the detection ability using various influenza A (pH1N1, H3N2, H5N2, and H6N5) viruses and influenza B virus-infected cells. RNA samples were extracted from cells infected with each virus for 1 h as described above. As shown in Figure 5 and Figure S6, the F/F_0 value was observed in the miRNA of A549 cells infected with various influenza viruses, including influenza A (pH1N1, H3N2, H5N2, and H6N5) viruses and influenza B virus. As a result of miR-181c-5p analysis (Figure 5a and Figure S6a), the F/F_0 values of pH1N1 virus-infected cells and infected cells of other viruses increased compared to mock-infected cells, and the highest response was observed in H6N5 virus infection. Recently, members of the miR-181 family (miR-181a−d) have been identified to control immune responses in infectious diseases by promoting B-cell differentiation.[56,57] The analysis of miR-181c-5p allows for the recognition of pathogen invasion, but there are limits to the selective detection of pH1N1 infection. The miR-1254 analysis generated the highest signal only in pH1N1 infection, whereas in other virus infections, the fluorescence signals were similar to those of mock-infected cells (control) (Figure 5b and Figure S6b). We analyzed miR-181c-5p and miR-1254 using dual-module CIVD kits and confirmed that the proposed systems could selectively distinguish pH1N1 infection from other influenza strains.

CONCLUSIONS

In this report, we suggested two species of miRNA as novel clinical biomarkers of influenza A virus infection and established a highly sensitive CIVD system. We studied the miRNA expression profile of the pH1N1-infected A549 cell line by using a microarray assay and qPCR and identified two miRNAs, hsa-miR-181c-5p and hsa-miR-1254, that can be used as diagnostic indicators for the detection of infectious disease. To detect these miRNAs, we designed programmed metastable hairpin probes and fixed the reporter probes on the sensing plate by using the strong affinity of avidin−biotin interaction. The fluorescence signal was amplified by hybridization of two types of hairpin probes to detect the target miRNA. Our proposed CIVD systems can detect subnanomolar amounts of target miRNAs without protein enzymes and thermal cycling steps and have the selectivity to distinguish even a single-base mismatch. In addition, we confirmed the detection performance in real RNA samples and compared it with the performance in other virus infections. Finally, we developed highly sensitive miRNA detection methods that could be potential diagnostic tools for pH1N1 infection by dual-module analysis of the expression of miR-181c-5p and miR-1254.

EXPERIMENTAL DETAILS

Materials. RPMI-1640 medium (L-glutamine), fetal bovine serum (FBS), Dulbecco's phosphate buffered saline (DPBS), 0.25% trypsin−EDTA, and penicillin−streptomycin (P/S, 10,000 U/mL) were purchased from Gibco (U.S.A.). Tosyl phenylalanyl chloromethyl ketone (TPCK)-treated trypsin was purchased from Thermo Fisher Scientific. All oligonucleotides were obtained from Bioneer (Korea) and dissolved upon arrival in 1× TE buffer (pH 8.0, 10 mM Tris−HCl, 1 mM EDTA, Korea). The oligonucleotides were further diluted to a stock concentration of 100 μM and stored at −20 °C. The sequences of all oligonucleotides are provided in Table S1. A nuclease-free duplex buffer (1×) was purchased from Integrated DNA Technologies (IDT, U.S.A.). A carbonate−bicarbonate buffer, magnesium chloride solution (1 M), and SA (from *Streptomyces avidinii*) were purchased from Sigma (U.S.A.). miRNA isolation kits, the RT-PCR assay (miRNeasy Mini Kit (cat. #217004), miScript Primer Assays (miRBase accession nos. hsa-miR-181c-5p (MIMAT 0000258), hsa-miR-642a-3p (MIMAT 0020924), hsa-miR-1254 (MIMAT 0005905), hsa-miR-3188 (MIMAT 0015070), hsa-miR-3921 (MIMAT 0018196), hsa-miR-3935 (MIMAT 0018350), hsa-miR-4442 (MIMAT 0018960), hsa-miR-4684-3p (MIMAT 0019770), hsa-miR-5585-3p (MIMAT 0022286), hsa-miR-6126 (MIMAT 0024599), hsa-miR-8060 (MIMAT 0030987), and hsa-miR-8063 (MIMAT 0030990)), the miScript SYBR Green PCR Kit (cat. #218075), and the miScript II RT Kit (cat. #218161) were purchased from Qiagen (Germany). Ethanol was purchased from Millipore (U.S.A.). All influenza viruses (A/CA/07/2009 (pH1N1), A/Brisbane/10/2007 (H3N2), A/aquatic bird/Korea/w351/2008 (H5N2), A/aquatic bird/Korea/CN5/2009 (H6N5), and B/Victoria/Brisbane/60/2008)) were provided by the BioNano Health Guard Research Center (H-GUARD, Korea).

Cell Culture and Virus Infection Protocol. A549 cells (human lung epithelial cells, ATCC no. CCL-185) were grown in RPMI-1640 medium containing 5% FBS and 1% P/S at 37 °C in a humidified atmosphere with 5% CO_2. Following this incubation, cells (1×10^6 cells/well) were plated in 6-well culture plates and grown overnight before viral infection. A549 cells were infected with influenza viruses at multiplicities of infection (MOIs) of 1 after washing thrice in DPBS (1 MOI = 1 virus particle/cell). All viruses used in this study were quantified by qRT-PCR. Cells were coincubated with influenza viruses in serum-free RPMI-1640 medium containing 1% P/S and 1 μg/mL TPCK trypsin at 37 °C for 1 or 2 h. After virus infection, the cellular medium containing the virus was changed to a fresh culture medium. Virus-infected cells were further incubated for 12 h postinfection (p.i.) at 37 °C.

Screening miRNAs as Potential Biomarkers of Virus Infection Diseases. Virus-infected A549 cells along with their culture medium were transferred into 2 mL tubes. The mixture was centrifuged for 10 min at 3200*g*. After centrifugation, the supernatant was discarded, and total RNA was extracted from the pellet according to miRNeasy Mini Kit protocols (Qiagen). The concentration of extracted RNA was quantified by the NanoDrop 2000 (Thermo Fisher Scientific) and stored at −80 °C before use. For the exploration of biomarkers, extracted RNA was analyzed by nucleic acid analysis using microarray and qRT-PCR assays. miRNA microarray analysis was performed by Macrogen (Korea). The analysis method is briefly described as follows. The Affymetrix GeneChip miRNA 4.0 array process was executed according to the manufacturer's protocol. Before the assay, RNA purity and integrity were evaluated by an ND-1000 spectrophotometer (NanoDrop, Wilmington, U.S.A.) and an Agilent 2100 bioanalyzer (Agilent Technologies, Palo Alto, U.S.A.). A total of 1000 ng of RNA samples was labeled with the FlashTag biotin RNA labeling kit (Genisphere, Hatfield, PA, U.S.A.). The labeled RNA was quantified, fractionated, and hybridized to the miRNA microarray according to the standard procedures provided by the manufacturer. The labeled RNA was heated to 99 °C for 5 min and then to 45 °C for 5 min. RNA-array hybridization was performed with agitation at 60 rotations per minute for 16 h at

DOI: 10.1021/acsomega.9b01790
ACS Omega 2019, 4, 14560−14568

48 °C on an Affymetrix GeneChip Fluidics Station 450. The chips were washed and stained using a GeneChip Fluidics Station 450 (Affymetrix, Santa Clara, California, U.S.A.). The chips were then scanned with an Affymetrix GCS 3000 scanner (Affymetrix, Santa Clara, California, U.S.A.). Signal values were computed using the Affymetrix GeneChip Command Console software. To select the optimal miRNAs as biomarkers among the overexpressed miRNAs in the microarray analysis, we also performed a qRT-PCR assay. RNA extracted from virus-infected A549 cells was synthesized with cDNA using the miScript II RT Kit (Qiagen). The qRT-PCR assay was carried out according to the miScript SYBR Green PCR Kit protocol and performed using the CFX96 Touch Real-Time PCR detection system (BIO-RAD). All primers used in this study were obtained from Qiagen. The relative quantitation was calculated using $2^{-\Delta\Delta Cq}$ methods.[58]

Design of Hairpin Probes on the Detection Plate. HA and HB were designed based on the principle of the enzyme-free target recycling circuit system, CHA, according to the target miRNA sequences. The sequences of HA and HB are described in Table S1. For the immobilization of HA on the detection plate by avidin−biotin interaction, biotinylated HA (bHA) was synthesized by replacing one T present at the loop site with biotin-dT. Prior to the experiments, each probe (HA, bHA, and HB) was prepared by annealing (keeping at 90 °C for 5 min and then slowly cooling down to room temperature). Therefore, all probes were formed into hairpin structures and stored at −20 °C before use.

Immobilization of Biotinylated Hairpin A (bHA) on the Detection Plate. The SA solution was prepared by dissolving SA in a coating buffer (carbonate−bicarbonate buffer). This SA solution was added to a 96-well black bottom immune plate (SPL, Korea) and incubated at 4 °C overnight. After washing twice with PBS-T (PBS containing 0.05% v/v Tween-20), the prepared SA-coated plate was treated with bHA (100 nM−1 μM) and incubated at 37 °C for 90 min. After immobilization, the plate was washed twice with PBS-T.

Fluorescence Kinetics Measurement. HB was treated with HA (50 μL) or bHA immobilized on the plate up to 100 μL. Before synthetic RNA or real RNA sample testing, the fluorescence intensity of non-template-containing solutions (F_0) was measured. One hundred microliters of RNA sample was added to the detection plate. Each fluorescence intensity was measured every 20 min for 2 h (F) by a Cytation 5 plate reader (BioTek) (λ_{ex} = 484 nm, λ_{em} = 530 nm).

■ ASSOCIATED CONTENT

Supporting Information

The Supporting Information is available free of charge on the ACS Publications website at DOI: 10.1021/acsomega.9b01790.

Sequences of involved DNAs, method of cell infection, miRNA extraction from cells, miRNA expression assay using microarray analysis, evaluation of Mg^{2+} concentration in reaction buffer, measurement of fluorescence kinetics (PDF)

■ AUTHOR INFORMATION

Corresponding Authors

*E-mail: jjung@kribb.re.kr (J.J.).
*E-mail: kangtaejoon@kribb.re.kr (T.K.).
*E-mail: eklim1112@kribb.re.kr (E.-K.L.).

ORCID

Taejoon Kang: 0000-0002-5387-6458
Eun-Kyung Lim: 0000-0003-2793-3700

Author Contributions

E-K.L., J.J., and T.K. conceived the idea and designed the experiments. J.L. and J.B. performed the microRNA screening experiments. P.K.B. and S.G.H. performed the cell and virus experiments. K.G. and J.L. analyzed the experimental data. E-K.L. and J.L. wrote the manuscript. All authors reviewed final version of the manuscript.

Notes

The authors declare no competing financial interest.

■ ACKNOWLEDGMENTS

This work was supported by the Center for BioNano Health Guard funded by the Ministry of Science and ICT (MSIT) as Global Frontier Project (nos. H-GUARD_2014-M3A6B2060507 and HGUARD_2013M3A6B2078950), the Bio & Medical Technology Development Program of the National Research Foundation (NRF) funded by MSIT (no. NRF-2018M3A9E2022821), the Basic Science Research Program of the NRF funded by MSIT (NRF2018R1C1B6005424), and the KRIBB Research Initiative Program.

■ ABBREVIATIONS

HA, hairpin probe A
HB, hairpin probe B
bHA, biotinylated hairpin probe A
SA, streptavidin
CHA, catalytic hairpin assembly
qRT-PCR, quantitative real-time PCR
CIVD, CHA-based in vitro diagnostic

■ REFERENCES

(1) Smith, D. J.; Lapedes, A. S.; de Jong, J. C.; Bestebroer, T. M.; Rimmelzwaan, G. F.; Osterhaus, A. D. M. E.; Fouchier, R. A. M. Mapping the antigenic and genetic evolution of influenza virus. *Science* **2004**, *305*, 371−376.

(2) Fan, N.; Wang, J. MicroRNA 34a contributes to virus-mediated apoptosis through binding to its target gene Bax in influenza A virus infection. *Biomed. Pharmacother.* **2016**, *83*, 1464−1470.

(3) Ojha, R.; Nandani, R.; Pandey, R. K.; Mishra, A.; Prajapati, V. K. Emerging role of circulating microRNA in the diagnosis of human infectious diseases. *J. Cell. Physiol.* **2019**, *234*, 1030−1043.

(4) Terrier, O.; Textoris, J.; Carron, C.; Marcel, V.; Bourdon, J. C.; Rosa-Calatrava, M. Host microRNA molecular signatures associated with human H1N1 and H3N2 influenza A viruses reveal an unanticipated antiviral activity for miR-146a. *J. Gen. Virol.* **2013**, *94*, 985−995.

(5) Vemula, S.; Zhao, J.; Liu, J.; Wang, X.; Biswas, S.; Hewlett, I. Current Approaches for Diagnosis of Influenza Virus Infections in Humans. *Viruses* **2016**, *8*, 96.

(6) Ge, Y.; Zhou, Q.; Zhao, K.; Chi, Y.; Liu, B.; Min, X.; Shi, Z.; Zou, B.; Cui, L. Detection of influenza viruses by coupling multiplex reverse-transcription loop-mediated isothermal amplification with cascade invasive reaction using nanoparticles as a sensor. *Int. J. Nanomed.* **2017**, *12*, 2645−2656.

(7) Lim, E. K.; Guk, K.; Kim, H.; Chung, B. H.; Jung, J. Simple, rapid detection of influenza A (H1N1) viruses using a highly sensitive peptide-based molecular beacon. *Chem. Commun.* **2016**, *52*, 175−178.

(8) Kumar, S.; Henrickson, K. J. Update on influenza diagnostics: lessons from the novel H1N1 influenza A pandemic. *Clin. Microbiol. Rev.* **2012**, *25*, 344−361.

DOI: 10.1021/acsomega.9b01790
ACS Omega 2019, 4, 14560−14568

(9) Catuogno, S.; Esposito, C. L.; Quintavalle, C.; Cerchia, L.; Condorelli, G.; De Franciscis, V. Recent Advance in Biosensors for microRNAs Detection in Cancer. *Cancers* **2011**, *3*, 1877−1898.
(10) Mackay, I. M.; Arden, K. E.; Nitsche, A. Real-time PCR in virology. *Nucleic Acids Res.* **2002**, *30*, 1292−1305.
(11) Shu, B.; Wu, K. H.; Emery, S.; Villanueva, J.; Johnson, R.; Guthrie, E.; Berman, L.; Warnes, C.; Barnes, N.; Klimov, A.; Lindstrom, S. Design and performance of the CDC real-time reverse transcriptase PCR swine flu panel for detection of 2009 A (H1N1) pandemic influenza virus. *J. Clin. Microbiol.* **2011**, *49*, 2614−2619.
(12) Li, Y.; Chan, E. Y.; Li, J.; Ni, C.; Peng, X.; Rosenzweig, E.; Tumpey, T. M.; Katze, M. G. MicroRNA expression and virulence in pandemic influenza virus-infected mice. *J. Virol.* **2010**, *84*, 3023−3032.
(13) Peng, F.; He, J.; Loo, J. F. C.; Kong, S. K.; Li, B.; Gu, D. Identification of serum MicroRNAs as diagnostic biomarkers for influenza H7N9 infection. *Virol. Rep.* **2017**, *7*, 1−8.
(14) Song, L.; Liu, H.; Gao, S.; Jiang, W.; Huang, W. Cellular microRNAs inhibit replication of the H1N1 influenza A virus in infected cells. *J. Virol.* **2010**, *84*, 8849−8860.
(15) Peng, F.; He, J.; Loo, J. F. C.; Yao, J.; Shi, L.; Liu, C.; Zhao, C.; Xie, W.; Shao, Y.; Kong, S. K.; Gu, D. Identification of microRNAs in throat swab as the biomarkers for diagnosis of influenza. *Int. J. Med. Sci.* **2016**, *13*, 77.
(16) Tambyah, P. A.; Sepramaniam, S.; Ali, J. M.; Chai, S. C.; Swaminathan, P.; Armugam, A.; Jeyaseelan, K. microRNAs in circulation are altered in response to influenza A virus infection in humans. *PLoS One* **2013**, *8*, No. e76811.
(17) Loo, J. F. C.; Wang, S. S.; Peng, F.; He, J. A.; He, L.; Guo, Y. C.; Gu, D. Y.; Kwok, H. C.; Wu, S. Y.; Ho, H. P.; Xie, W. D.; Shao, Y. H.; Kong, S. K. A non-PCR SPR platform using RNase H to detect MicroRNA 29a-3p from throat swabs of human subjects with influenza A virus H1N1 infection. *Analyst* **2015**, *140*, 4566−75.
(18) Chen, Z.; Liang, H.; Chen, X.; Ke, Y.; Zhou, Z.; Yang, M.; Zen, K.; Yang, R.; Liu, C.; Zhang, C. Y. An Ebola virus-encoded microRNA-like fragment serves as a biomarker for early diagnosis of Ebola virus disease. *Cell Res.* **2016**, *26*, 380−383.
(19) Deng, R.; Zhang, K.; Li, J. Isothermal Amplification for MicroRNA Detection: From the Test Tube to the Cell. *Acc. Chem. Res.* **2017**, *50*, 1059−1068.
(20) Ko, H. Y.; Lee, J.; Joo, J. Y.; Lee, Y. S.; Heo, H.; Ko, J. J.; Kim, S. A color-tunable molecular beacon to sense miRNA-9 expression during neurogenesis. *Sci. Rep.* **2014**, *4*, 4626.
(21) Tang, X.; Deng, R.; Sun, Y.; Ren, X.; Zhou, M.; Li, J. Amplified Tandem Spinach-Based Aptamer Transcription Enables Low Background miRNA Detection. *Anal. Chem.* **2018**, *90*, 10001−10008.
(22) Kim, D.; Wei, Q.; Kim, D. H.; Tseng, D.; Zhang, J.; Pan, E.; Garner, O.; Ozcan, A.; Di Carlo, D. Enzyme-Free Nucleic Acid Amplification Assay Using a Cellphone-Based Well Plate Fluorescence Reader. *Anal. Chem.* **2018**, *90*, 690−695.
(23) Kim, H.; Kang, S.; Park, K. S.; Park, H. G. Enzyme-free and label-free miRNA detection based on target-triggered catalytic hairpin assembly and fluorescence enhancement of DNA-silver nanoclusters. *Sens. Actuators, B* **2018**, *260*, 140−145.
(24) Kolpashchikov, D. M. An elegant biosensor molecular beacon probe: challenges and recent solutions. *Scientifica* **2012**, *2012*, 928783.
(25) Tian, T.; Wang, J.; Zhou, X. A review: microRNA detection methods. *Org. Biomol. Chem.* **2015**, *13*, 2226−2238.
(26) Válóczi, A.; Hornyik, C.; Varga, N.; Burgyán, J.; Kauppinen, S.; Havelda, Z. Sensitive and specific detection of microRNAs by northern blot analysis using LNA-modified oligonucleotide probes. *Nucleic Acids Res.* **2004**, *32*, No. e175.
(27) Yan, L.; Zhou, J.; Zheng, Y.; Gamson, A. S.; Roembke, B. T.; Nakayama, S.; Sintim, H. O. Isothermal amplified detection of DNA and RNA. *Mol. BioSyst.* **2014**, *10*, 970−1003.
(28) Zhao, Y.; Chen, F.; Li, Q.; Wang, L.; Fan, C. Isothermal Amplification of Nucleic Acids. *Chem. Rev.* **2015**, *115*, 12491−12545.
(29) Neubacher, S.; Arenz, C. Rolling-Circle Amplification: Unshared Advantages in miRNA Detection. *ChemBioChem* **2009**, *10*, 1289−1291.
(30) Zhuang, J.; Lai, W.; Chen, G.; Tang, D. A rolling circle amplification-based DNA machine for miRNA screening coupling catalytic hairpin assembly with DNAzyme formation. *Chem. Commun.* **2014**, *50*, 2935−2938.
(31) Jiang, Y.; Li, B.; Milligan, J. N.; Bhadra, S.; Ellington, A. D. Real-time detection of isothermal amplification reactions with thermostable catalytic hairpin assembly. *J. Am. Chem. Soc.* **2013**, *135*, 7430−7433.
(32) Zhang, Y.; Yan, Y.; Chen, W.; Cheng, W.; Li, S.; Ding, X.; Li, D.; Wang, H.; Ju, H.; Ding, S. A simple electrochemical biosensor for highly sensitive and specific detection of microRNA based on mismatched catalytic hairpin assembly. *Biosens. Bioelectron.* **2015**, *68*, 343−349.
(33) Ge, Z.; Lin, M.; Wang, P.; Pei, H.; Yan, J.; Shi, J.; Huang, Q.; He, D.; Fan, C.; Zuo, X. Hybridization chain reaction amplification of microRNA detection with a tetrahedral DNA nanostructure-based electrochemical biosensor. *Anal. Chem.* **2014**, *86*, 2124−2130.
(34) Yang, C.; Shi, K.; Dou, B.; Xiang, Y.; Chai, Y.; Yuan, R. In situ DNA-templated synthesis of silver nanoclusters for ultrasensitive and label-free electrochemical detection of microRNA. *ACS Appl. Mater. Interfaces* **2015**, *7*, 1188−1193.
(35) Miao, J.; Wang, J.; Guo, J.; Gao, H.; Han, K.; Jiang, C.; Miao, P. A plasmonic colorimetric strategy for visual miRNA detection based on hybridization chain reaction. *Sci. Rep.* **2016**, *6*, 32219.
(36) Li, C.; Li, Z.; Jia, H.; Yan, J. One-step ultrasensitive detection of microRNAs with loop-mediated isothermal amplification (LAMP). *Chem. Commun.* **2011**, *47*, 2595−2597.
(37) Liang, C. P.; Ma, P. Q.; Liu, H.; Guo, X.; Yin, B. C.; Ye, B. C. Rational Engineering of a Dynamic, Entropy-Driven DNA Nanomachine for Intracellular MicroRNA Imaging. *Angew. Chem., Int. Ed* **2017**, *56*, 9077−9081.
(38) Yang, L.; Wu, Q.; Chen, Y.; Liu, X.; Wang, F.; Zhou, X. Amplified MicroRNA Detection and Intracellular Imaging Based on an Autonomous and Catalytic Assembly of DNAzyme. *ACS Sens.* **2019**, *4*, 110−117.
(39) Chang, C. C.; Wang, G.; Takarada, T.; Maeda, M. Target-Recycling-Amplified Colorimetric Detection of Pollen Allergen Using Non-Cross-Linking Aggregation of DNA-Modified Gold Nanoparticles. *ACS Sens.* **2019**, *4*, 363−369.
(40) Li, Q.; Zeng, F.; Lyu, N.; Liang, J. Highly sensitive and specific electrochemical biosensor for microRNA-21 detection by coupling catalytic hairpin assembly with rolling circle amplification. *Analyst* **2018**, *143*, 2304−2309.
(41) Miao, X.; Ning, X.; Li, Z.; Cheng, Z. Sensitive detection of miRNA by using hybridization chain reaction coupled with positively charged gold nanoparticles. *Sci. Rep.* **2016**, *6*, 32358.
(42) Wu, X.; Chai, Y.; Zhang, P.; Yuan, R. An electrochemical biosensor for sensitive detection of microRNA-155: combining target recycling with cascade catalysis for signal amplification. *ACS Appl. Mater. Interfaces* **2015**, *7*, 713−720.
(43) Qi, Y.; Li, Y.; Zhang, L.; Huang, J. microRNA expression profiling and bioinformatic analysis of dengue virusinfected peripheral blood mononuclear cells. *Mol. Med. Rep.* **2013**, *7*, 791−798.
(44) Kang, W. J.; Cho, Y. L.; Chae, J. R.; Lee, J. D.; Choi, K. J.; Kim, S. Molecular beacon-based bioimaging of multiple microRNAs during myogenesis. *Biomaterials* **2011**, *32*, 1915−1922.
(45) Eisfeld, A. J.; Neumann, G.; Kawaoka, Y. Influenza A virus isolation, culture and identification. *Nat. Protoc.* **2014**, *9*, 2663−2681.
(46) Lam, W.-Y.; Yeung, A. C.-M.; Ngai, K. L.-K.; Li, M.-S.; To, K.-F.; Tsui, S. K.-W.; Chan, P. K.-S. Effect of avian influenza A H5N1 infection on the expression of microRNA-141 in human respiratory epithelial cells. *BMC Microbiol.* **2013**, *13*, 104.
(47) Foss, K. M.; Sima, C.; Ugolini, D.; Neri, M.; Allen, K. E.; Weiss, G. J. miR-1254 and miR-574-5p: serum-based microRNA biomarkers for early-stage non-small cell lung cancer. *J. Thorac. Oncol.* **2011**, *6*, 482−488.

DOI: 10.1021/acsomega.9b01790
ACS Omega 2019, 4, 14560−14568

(48) Pu, M.; Li, C.; Qi, X.; Chen, J.; Wang, Y.; Gao, L.; Miao, L.; Ren, J. MiR-1254 suppresses HO-1 expression through seed region-dependent silencing and non-seed interaction with TFAP2A transcript to attenuate NSCLC growth. *PLoS Genet.* **2017**, *13*, No. e1006896.
(49) Meliopoulos, V. A.; Andersen, L. E.; Brooks, P.; Yan, X.; Bakre, A.; Coleman, J. K.; Tompkins, S. M.; Tripp, R. A. MicroRNA regulation of human protease genes essential for influenza virus replication. *PLoS One* **2012**, *7*, No. e37169.
(50) Kumar, A.; Muhasin, A. V. N.; Raut, A. A.; Sood, R.; Mishra, A. Identification of Chicken Pulmonary miRNAs Targeting PB1, PB1-F2, and N40 Genes of Highly Pathogenic Avian Influenza Virus H5N1 In Silico. *Bioinf. Biol. Insights* **2014**, *8*, 135−145.
(51) Foo, C. H.; Rootes, C. L.; Cowley, K.; Marsh, G. A.; Gould, C. M.; Deffrasnes, C.; Cowled, C. J.; Klein, R.; Riddell, S. J.; Middleton, D.; Simpson, K. J.; Wang, L.-F.; Bean, A. G. D.; Stewart, C. R. Dual microRNA Screens Reveal That the Immune-Responsive miR-181 Promotes Henipavirus Entry and Cell-Cell Fusion. *PLoS Pathog.* **2016**, *12*, e1005974.
(52) Skalsky, R. L.; Cullen, B. R. Viruses, microRNAs, and host interactions. *Annu. Rev. Microbiol.* **2010**, *64*, 123−141.
(53) Qiu, L.; Wu, C.; You, M.; Han, D.; Chen, T.; Zhu, G.; Jiang, J.; Yu, R.; Tan, W. A targeted, self-delivered, and photocontrolled molecular beacon for mRNA detection in living cells. *J. Am. Chem. Soc.* **2013**, *135*, 12952−12955.
(54) Zheng, J.; Yang, R.; Shi, M.; Wu, C.; Fang, X.; Li, Y.; Li, J.; Tan, W. Rationally designed molecular beacons for bioanalytical and biomedical applications. *Chem. Soc. Rev.* **2015**, *44*, 3036−3055.
(55) Moraitis, M. I.; Xu, H.; Matthews, K. S. Ion concentration and temperature dependence of DNA binding: comparison of PurR and LacI repressor proteins. *Biochemistry* **2001**, *40*, 8109−8117.
(56) Merkerova, M.; Belickova, M.; Bruchova, H. Differential expression of microRNAs in hematopoietic cell lineages. *Eur. J. Haematol.* **2008**, *81*, 304−310.
(57) Shi, L.; Cheng, Z.; Zhang, J.; Li, R.; Zhao, P.; Fu, Z.; You, Y. hsa-mir-181a and hsa-mir-181b function as tumor suppressors in human glioma cells. *Brain Res.* **2008**, *1236*, 185−193.
(58) Makkoch, J.; Poomipak, W.; Saengchoowong, S.; Khongnomnan, K.; Praianantathavorn, K.; Jinato, T.; Poovorawan, Y.; Payungporn, S. Human microRNAs profiling in response to influenza A viruses (subtypes pH1N1, H3N2, and H5N1). *Exp. Biol. Med.* **2016**, *241*, 409−420.

DOI: 10.1021/acsomega.9b01790
ACS Omega 2019, 4, 14560−14568